Article

Study of Geopolymer Composites Based on Volcanic Ash, Fly Ash, Pozzolan, Metakaolin and Mining Tailing

Rossibel Churata [1], Jonathan Almirón [2,*], María Vargas [3], Danny Tupayachy-Quispe [3], Jeniffer Torres-Almirón [3], Yosheff Ortiz-Valdivia [2] and Francisco Velasco [4]

1   Escuela Profesional de Ingeniería de Materiales, Facultad de Ingeniería de Procesos, Universidad Nacional de San Agustín de Arequipa, Calle Santa Catalina Nro. 117 Cercado, Arequipa 04001, Peru; rchurataa@unsa.edu.pe
2   Escuela Profesional de Ingeniería Ambiental, Facultad de Ingeniería de Procesos, Universidad Nacional de San Agustín de Arequipa, Calle Santa Catalina Nro. 117 Cercado, Arequipa 04001, Peru; yortizv@unsa.edu.pe
3   Laboratorio de Ciencia de los Materiales, Facultad de Ciencias e Ingenierías Físicas y Formales, Universidad Católica de Santa María, Samuel Velarde 320, Arequipa 04000, Peru; mvargasv@ucsm.edu.pe (M.V.); dtupayachy@ucsm.edu.pe (D.T.-Q.); jeniffer.torres@ucsm.edu.pe (J.T.-A.)
4   Materials Science and Engineering Department, IAAB, Universidad Carlos III de Madrid, 28005 Madrid, Spain; fvelasco@ing.uc3m.es
*   Correspondence: jalmiron@unsa.edu.pe

Abstract: This work studies the feasibility to employ a combination of volcanic ash (natural waste) with different raw materials in the production of geopolymers: fly ash and mining tailing (considered hazardous solid waste), natural pozzolan, and metakaolin. This study compares the properties of geopolymers based on volcanic ash with fly ash, pozzolan, metakaolin, and mining tailing in a relation of 1:1 with the addition of NaOH 15M and Na_2SiO_3 as alkali activators. FTIR and XRD assays and mechanical tests were employed to characterize the geopolymers. The results showed that those materials can be used as raw materials to produce geopolymers. Additionally, the results revealed that prime material composition and their mineralogical characteristics influence the geopolymerization reaction and compression strength, reaching values of 35 MPa for the volcanic ash-pozzolan mixture. The pozzolan is a good source of Al_2O_3 and SiO_2 and is highly reactive to the alkali activators resulting in a better geopolymerization in comparison to the mixtures of volcanic ash with metakaolin, fly ash, or mining tailing.

1. Introduction

Geopolymers (GP) are inorganic polymers formed by the polycondensation of an amorphous solid aluminosilicate in an alkali medium (hydroxide or silicate from an alkaline metal) through a geopolymerization process [1]. This reaction yields an amorphous three-dimensional structure in which SiO_4 and AlO_4 tetrahedra are linked by corner-shared O atoms. Raw materials such as metakaolin [2,3], fly ash [4], pozzolan [5], or volcanic ash [6–9], alongside with alkali solutions (NaOH or KOH with the addition of Na_2SiO_3), are used in the synthesis of geopolymers. The reaction mechanisms that occur during the formation of geopolymers depend on the chemical composition of the raw materials, the activating solution, and synthesis conditions; for example, there are slags rich in silicon, calcium, and aluminum; and the ash and metakaolin are rich in silicon and aluminum. In the case of slag due to calcium, the calcium silicate hydrate (CSH) is mainly produced; while using ash and metakaolin, amorphous aluminosilicates with three-dimensional structures are generated [10]. The reaction mechanism is not yet clear, but a model proposed by Provis mentions that the first thing that happens is the dissolution of aluminosilicates in

monomers and then, they precipitate in the form of aluminosilicate gels because the Al-O are weaker than Si-O bonds. Subsequently, the reorganization process occurs that consists of the incorporation of silicon (which influences the mechanical properties) and finally, polymerization and hardening [10].

In the last years, several studies have studied geopolymers as a potential substitute for Portland cement (PC), in order to reduce the emissions of CO_2 to the environment that comes from PC production, and subsequently reduce the carbon footprint [6,11,12]. Among other applications of geopolymer are in precast applications, in the production of railway sleepers and sewer pipes, in structural elements such as columns beans and tunnel segments, and in passive building [13]. Besides, the properties of geopolymer concrete could be used to produce durable structures, repair materials (for instance, in highway infrastructures but it is still limited to light pavement applications), piers, coastal bridges, and underwater concrete supports that are exposed to harsh environments such as sulphate soils, chloride corrosion, attack from saltwater. So, their potential applications depend on their properties and there are some studies that used them in highway pavement applications and as a covering material so the concrete structures could be protected from the marine environment; however, further investigations are needed [13]. Geopolymers are well known to have good binding and mechanical properties [6,14], low shrinkage, thermal stability, freeze–thaw, chemical and fire resistance, long-term durability, and recyclability [15]; being one of the advantages of the production of geopolymers the origin of raw materials, because aluminosilicates can be found as industrial by-products such as fly ash [4,16], phosphate mine tailing [17], and blast furnace slag [18], or as natural materials such as kaolin [16], metakaolin [3,19], clay, and volcanic ash [7–9], among others. Therefore, these several sources used for their synthesis generate the following types of geopolymers based on fly ash, metakaolin, slag, rice husk ash, high calcium wood ash, and a combination of two or three different sources [10].

Some of the main factors identified that contribute to the formation and properties of geopolymers are binder content, alkali activators, starting aluminosilicate constituents or aluminosilicate, alkali activator solution ratio, binder ratio, molarity, aggregates, fineness, additional water, curing conditions, among others [20]. Of the constituents or starting aluminosilicate, it is important to consider the mineralogical composition, chemistry, particle size, glassy phase content, and particle morphology, as they have an important effect on geopolymerization activity and reactions [21]. It is known that the mechanical properties of geopolymers are influenced by the chemical composition of the raw materials and activators [22]. The addition of two or more raw materials-aluminosilicates in the geopolymer production could result in a geopolymer with better properties than those with one raw material-aluminosilicate [23]. There are different sources of materials with high alumina and silica content to produce geopolymers. For that reason, it is possible to combine different raw materials-aluminosilicates to improve the physical and mechanical properties, or to obtain geopolymers with a lower SiO_2/Al_2O_3 molar ratio. Zhen et al. [24] reported that a lower SiO_2/Al_2O_3 molar ratio shifts the pore distribution of geopolymers into smaller pores, decreasing the surface area of the material, affecting leaching and heavy metal immobilization. According to Ma et al. [25], the workability of geopolymer concrete depends on the activator molarity, superplasticizer, and water content. So, the mechanism of action depends on the raw material, geopolymer concrete properties, activator solutions used, and synthesis conditions. For instance, when a geopolymer concrete is attacked by an acid, its response depends on the acid strength, concentration of the activator solution used, exposure time, mineralogical composition, and its properties. Besides, it has been seen that a fly ash-based geopolymer concrete activated by NaOH solution has the best acid resistance and this is probably due to Na that reacts with these acids and produces hydrated salts [25].

Fly ash is a fine powder by-product transported by flue gas after the combustion of coal in coal-fired power stations typically made up of small glass spheres, consisting primarily of silicon, aluminum, iron, and calcium oxides [26]. However, fly ash-based

geopolymers typically exhibit brittle behavior with low tensile strength, ductility, and fracture toughness, thus limiting up to now the actual possibility to use these very promising materials for extensive and practical applications in constructions. This limit could be, in principle, overcome by developing geopolymer composites, but, to the best of our knowledge, very little is reported on this topic [15]. The microstructure, porosity, and degree of densification of geopolymers depend on temperature [27]. Resistance at high temperatures is an important characteristic of construction materials, in the case of fire; in this sense, studies of geopolymers indicate that compressive strength increases at high temperatures (>600 °C), so geopolymer composites are generally considered thermal and fire-resistant structures [28].

Volcanic ash is an aluminosilicate material with Al_2O_3 and SiO_2 contents that make the synthesis of geopolymers possible [7–9]. There are eight active volcanoes located in the south of Peru [29], where the most active volcano is the Ubinas (16° 22′ S, 70° 54′ W; 5672 m above sea level—asl) with a recurrence of four to seven unrest episodes per century [30]. The activity of the Ubinas Volcano has generated millions of tons of volcanic material resulting in deposits with a mafic andesitic composition [31], which can be used in the production of geopolymers [8] with a positive economic impact on the country.

This paper aims to explore the feasibility of using volcanic ash in combination with different raw materials in the production of geopolymers (e.g., fly ash, pozzolan, kaolin, and mining tailing). A study of volcanic ashes, fly ashes, and mining wastes is proposed, due to the fact that these are usually deposited in landfills that generate environmental problems, so it is intended to valorize this type of waste. Additionally, because in this research volcanic ash mixtures are studied in combination with different raw materials, it is important to analyze the behavior of these new mixtures because the modification of the starting components also changes the results. For instance, the amount of Al in a geopolymer reaction plays an important role in the curing time and compressive strength. Therefore, reducing the amount of Al leads to longer curing times, and when the amount of Al increases the compressive strength is lower [32]. In addition, the amorphous and crystalline phase content of the raw materials influences the compressive strength results, amorphous phases dissolve more easily than crystalline phases during geopolymerization [2].

On the other hand, it is also intended to evaluate the influence that the introduction of pozzolan and kaolin has on the mechanical properties of geopolymers with volcanic ashes. The geopolymers obtained have been characterized by the techniques: X-ray diffraction (XRD), FTIR analysis, and compressive strength tests, to determine their suitability for construction applications.

2. Materials and Methods

2.1. Materials

The volcanic ash (Vol) employed in this work comes from Ubinas Volcano, located in Moquegua (Peru), which was taken from a location with the coordinates: latitude 297,608 m, length 8,196,158 m, and 4600 m asl. This volcanic ash is considered a natural waste. The fly ash (Fly) was obtained from the thermal power plant ILO2_ENERSUR located in Moquegua (Peru). Kaolin was obtained from the company Agregados Calcáreos S.A. with a particle size of 99.9991% under 38 μm. The pozzolan (Pz) was obtained from Yura, located in Arequipa (Peru). The mining tailing (Mt) was supplied by the CANDEL IV mine, located in Yarabamba, Arequipa (Peru).

The portions of volcanic ash, pozzolan, and mining tailing were grounded in a Fritsch planetary ball mill model Pulverisette 6 to obtain a particle size lower than 70 μm. The portion of kaolin was calcined in an electric furnace (Nabertherm) at 750 °C for 3 h, with a heating rate of 5 °C/min [2] to obtain a high reactive metakaolin (Mk).

The alkali activator applied in this work consisted of 25% of Na_2SiO_3 and 75% NaOH (99% purity). The liquid portions of mixtures were NaOH 15M and Na_2SiO_3 with a composition of 18% Na_2O, 32.12% SiO_2, and 55.01% H_2O. The alkali activation solution was premixed and settled for 24 h at room temperature.

The raw materials that were grounded in a Fritsch planetary ball mill model Pulverisette 6 to obtain a particle size lower than 70 μm were characterized through X-ray fluorescence and X-ray diffraction assays. The chemical composition of the raw materials-aluminosilicates was analyzed through X-ray fluorescence, employing Spectro Xepos equipment. Table 1 shows the results. Mineralogical analysis was conducted via X-ray powder diffraction (XRD). The sample A diffractometer Bruker D8, radiation source CuKα (λ = 0.1542 nm), 40 kV, and 40 mA were employed to obtain the XRD diffractograms of Vol, Fly, Pz, Mk, and Mt. Samples were analyzed at 2θ angles between 10° and 80° with a scanning rate of 2°/min. The diffractograms show that Pz has the largest amount of amorphous particles followed by Mk, Fly, Vol, and Mt. The crystalline phases detected in Pz are quartz, aluminum hydroxide, and silicon oxide; Mk contains quartz and kaolinite; Fly contains quartz, mullite, and calcite; Vol contains anorthite and quartz; and Mt contains quartz, mullite, calcite, copper phosphate trihydrate, iron phosphate, and aluminum hydroxide with silicon oxide. As it was noted, when quartz (SiO_2) is present in all of the raw materials, the geopolymerization process slows down due to its hard dissolution in an alkali solution [33]. The Mk obtained at temperatures of 600 °C to 900 °C can improve the chemical reactivity of kaolinite [34].

Table 1. Chemical composition of volcanic ash (Vol), fly ash (Fly), pozzolan (Pz), metakaolin (Mk), and mining tailings (Mt).

Oxide	Vol	Fly	Pz	Mk	Mt
SiO_2	44.91	44.44	53.11	42.78	45.54
Al_2O_3	13.30	25.75	10.16	30.91	12.99
Fe_2O_3	6.67	4.54	1.49	0.06	9.25
CaO	5.14	3.14	1.14	0.09	3.13
MgO	3.55	1.27	0.25	0.00	2.96
K_2O	1.47	1.80	2.68	0.58	1.12
Na_2O	0.26	0.01	0.01	0.01	0.01
P_2O_5	0.37	0.14	0.09	0.24	0.12
SO_3	0.36	0.54	0.09	0.24	0.89
TiO_2	1.07	1.13	0.22	0.35	0.41
CuO	0.00	0.01	0.00	0.00	0.44
LOI *	22.39	16.75	30.37	22.80	21.93

* LOI: loss on ignition.

2.2. Geopolymer Synthesis

The production of geopolymers consisted in the preparation of mixtures with 50% of volcanic ash and 50% of any of the other raw materials (Fly, Pz, Mk, and Mt), followed by the addition of the alkali activation solution for 5 min. The ratio for alkali solution/raw material was 0.16. The paste was poured into a cylindrical mold with a height:diameter ratio of 2:1 according to the EN 12504-1:2009 standard. The paste was compressed until 15 MPa, then samples were taken from the mold, covered by a thin polyethylene film to avoid the evaporation of water, and hardened at 80 °C for 48 h for curing. The compression strength test of five samples per each formulation was made after 7, 28, 60, and 90 days of curing at room temperature (24 ± 3 °C) employing an electro-hydraulic press (ELE International) with a loading rate of 10 mm/min according to the ASTM C39 standard. The design of geopolymer paste composition is shown in Table 2.

Table 2. Geopolymer paste composition, based on volcanic ash with fly ash, pozzolan, metakaolin, and mining tailing.

Formulation Label	SiO_2	Al_2O_3	SiO_2/Al_2O_3	Solid/Liquid Ratio
Fly-Vol	44.68	19.53	3.88	0.16
Pz-Vol	49.01	11.73	7.09	0.16
Mk-Vol	43.85	22.11	3.37	0.16
Mt-Vol	44.91	13.15	5.73	0.16

After the compression test, the pieces of samples were grounded and stored for XRD and FTIR analysis. The FTIR analysis was made with the powder of prime material and geopolymer samples in a Spectrum GX FT-IR Perkin-Elmer spectrometer using Spectrum v2:00 software. XRD was made at the same conditions previously mentioned in Section 2.1.

3. Results and Discussion

3.1. X-ray Diffraction Patterns of Geopolymers

A comparison of the XRD patterns of raw materials (Vol, Fly, Pz, Mk, and Mt) and geopolymers from different mixtures is shown in Figure 1. Figure 1A, corresponding to the mixture of fly ash (Fly) and volcanic ash (Vol), reveals that fly ash has a higher content of particles in the amorphous phase compared to the volcanic ash. It is also observed that, as a consequence of the activation process of Fly and Vol, there are changes in the intensity of the peaks. The main crystalline phases that originally existed in Fly and Vol are present in the geopolymers (except the calcite that reacted during the geopolymerization), indicating the presence of undissolved particles of volcanic ash and fly ash in the GP(Fly-Vol) geopolymers.

Figure 1B shows the XRD patterns of Pz and Vol raw materials and GP(Pz-Vol) geopolymers. Pz has a higher content of amorphous phase particles compared to volcanic ash. The mineral phases of Pz are not observed in the geopolymers, which suggests that Pz was able to completely dissolve in the alkaline solution and contribute to improving the properties of the geopolymerization because the diffuse halo peak located from 15°–40° (2θ) angles is seen in the Pz curve, indicating the presence of a thermodynamically metastable amorphous aluminosilicate structure with high pozzolanic activity. It is observed that the mineral phases contained in the volcanic ash are still present in the diffractograms of the sample GP(Pz-Vol), although a wide hump appears indicating the amorphous state.

Figure 1C shows the curves of Mk and Vol raw materials and GP(Mk-Vol) geopolymer. Mk has a higher content of particles in the amorphous phase compared to volcanic ash. Moreover, Mk includes a small amount of hardly soluble crystals (mainly quartz and kaolinite). Mk also shows a thermodynamically metastable amorphous aluminosilicate structure from 15°–40° (2θ) angles with high pozzolanic activity. The peaks of the mineral phases contained in the volcanic ash are still present in the diffractograms of the GP(Mk-Vol) geopolymer.

Figure 1D shows the mineralogical phases of Mt, Vol, and GP(Mt-Vol) geopolymer. The XRD pattern of Mt shows many crystalline phases such as quartz, mullite, calcite, copper phosphate trihydrate, iron phosphate, and aluminum hydroxide with silicon oxide, indicating that the composition of the mining tailing is more complex. The XRD pattern of the GP(Mt-Vol) geopolymer reveals the presence of an amorphous hump with a wide bottom at angles of 25°–40° (2θ); the sharp peaks of anorthite are still present in the geopolymer; and some remarkable peaks of Mt and Vol almost disappeared or decreased in intensity.
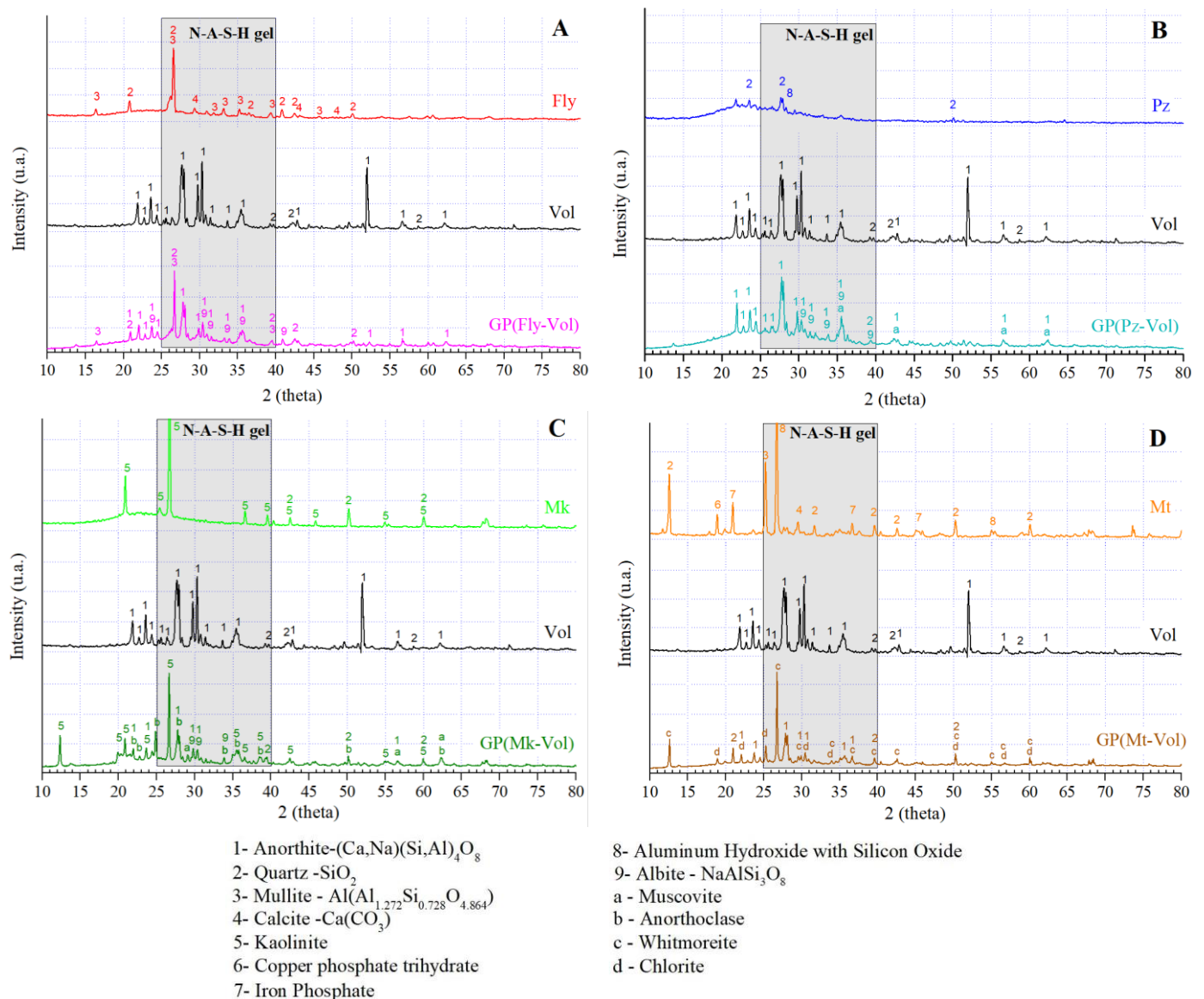
Figure 1. XRD patterns of raw materials (Vol, Fly, Pz, Mk, and Mt) and geopolymers. (**A**) Mineralogical phases of Fly, Vol, and GP(Fly-Vol). (**B**) Mineralogical phases of Pz, Vol, and GP(Pz-Vol). (**C**) Mineralogical phases of Mk, Vol, and GP(Mk-Vol). (**D**) Mineralogical phases of Mt, Vol, and GP(Mt-Vol).

The XRD patterns of the geopolymers based on volcanic ash with the other raw materials (Fly, Pz, Mk, or Mt) are shown in Figure 2. The amorphous glassy phase is observed in all the samples (regardless of the mixture of solids used) from 25°–40° (2θ angles). This halo is the result of the formation of an alkaline aluminosilicate gel (N-A-S-H gel), the main product in the reaction to produce geopolymers [19]. The highest intensity of the diffuse halo peak corresponds to the GP(Pz-Vol) geopolymer, followed by GP(Mk-Vol), GP(Fly-Vol), and GP(Mt-Vol). For that reason, it is inferred that geopolymers based on Pz have the highest amount of amorphous glassy phase. It is also observed that the mineral phases contained in the volcanic ash (anorthite and quartz) are still present in the diffractograms of all the geopolymers. This could be justified by the fact that these mineral phases have been unaltered or only partially dissolved in the alkaline medium. Therefore, these unreacted phases could act as microaggregates or fillers by reinforcing the geopolymer matrix, resulting in a compact and high-strength structure [35].
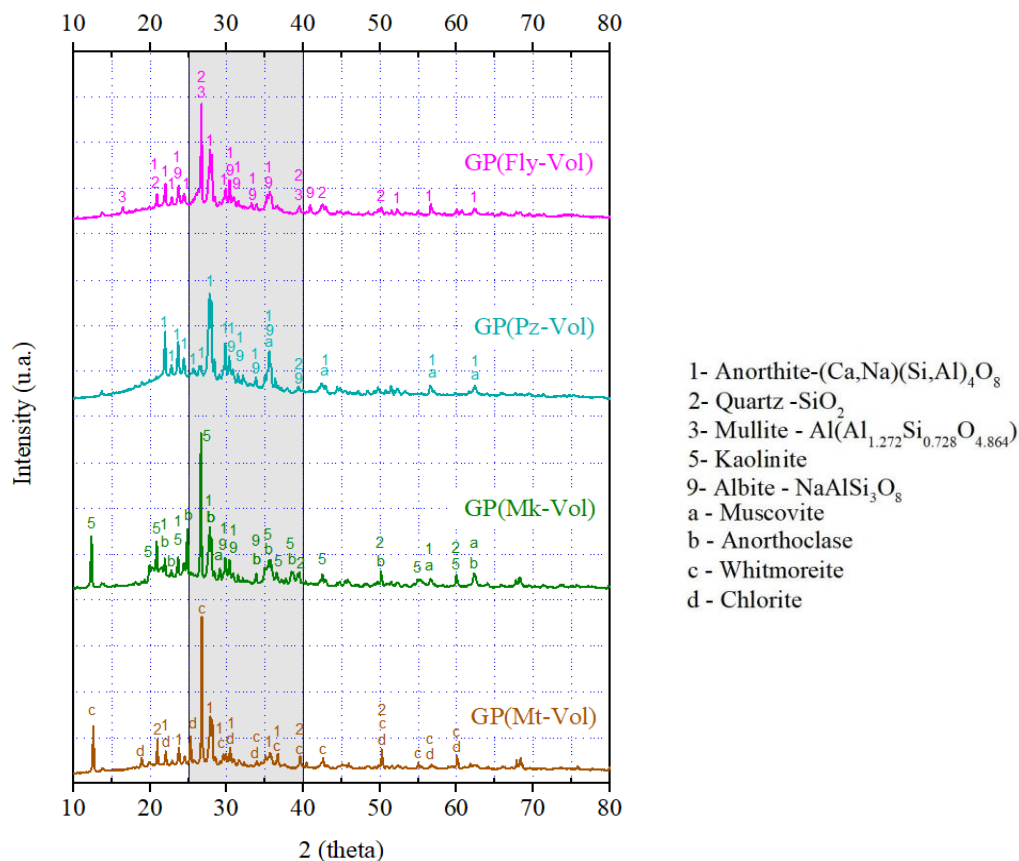
Figure 2. XRD patterns of geopolymers based on volcanic ash with the other raw materials (Fly, Pz, Mk, and Mt).

3.2. FTIR Spectra

The infrared spectra of raw materials and geopolymers are shown in Figure 3. The highest intensity peak corresponding to the adsorption band in the 1030 cm^{-1}–1090 cm^{-1} range can be related to the vibration of the asymmetric stretching of the Si-O-T bonds in TO_4 (T = Si or Al) [8,36,37] of the raw materials (Vol, Fly, Pz, Mk, and Mt). When comparing it with the rest of GP(Fly-Vol), GP(Pz-Vol), GP(Mk-Vol), and GP(Mt-Vol) geopolymers, a shift of this main band towards lower wavenumbers (from 912 cm^{-1}–1005 cm^{-1}) is observed, which is attributed to the increase in the tetrahedral aluminum related to the Si/Al ratio of the geopolymers [8]. By increasing the Al replacement degree (instead of Si), shown by this shifting of the band, the important role of the high content of aluminum in the formation of aluminosilicate gel is appreciated, having a positive impact on the enhancement of the geopolymerization [38]. Those results reveal the strong atomic bonds associated with the formation of a geopolymer gel [36,37]. Moreover, these bands correspond to the main part of the aluminosilicate matrix in the formation of a geopolymer, showing that the raw materials reacted to the alkali solution [37,38].
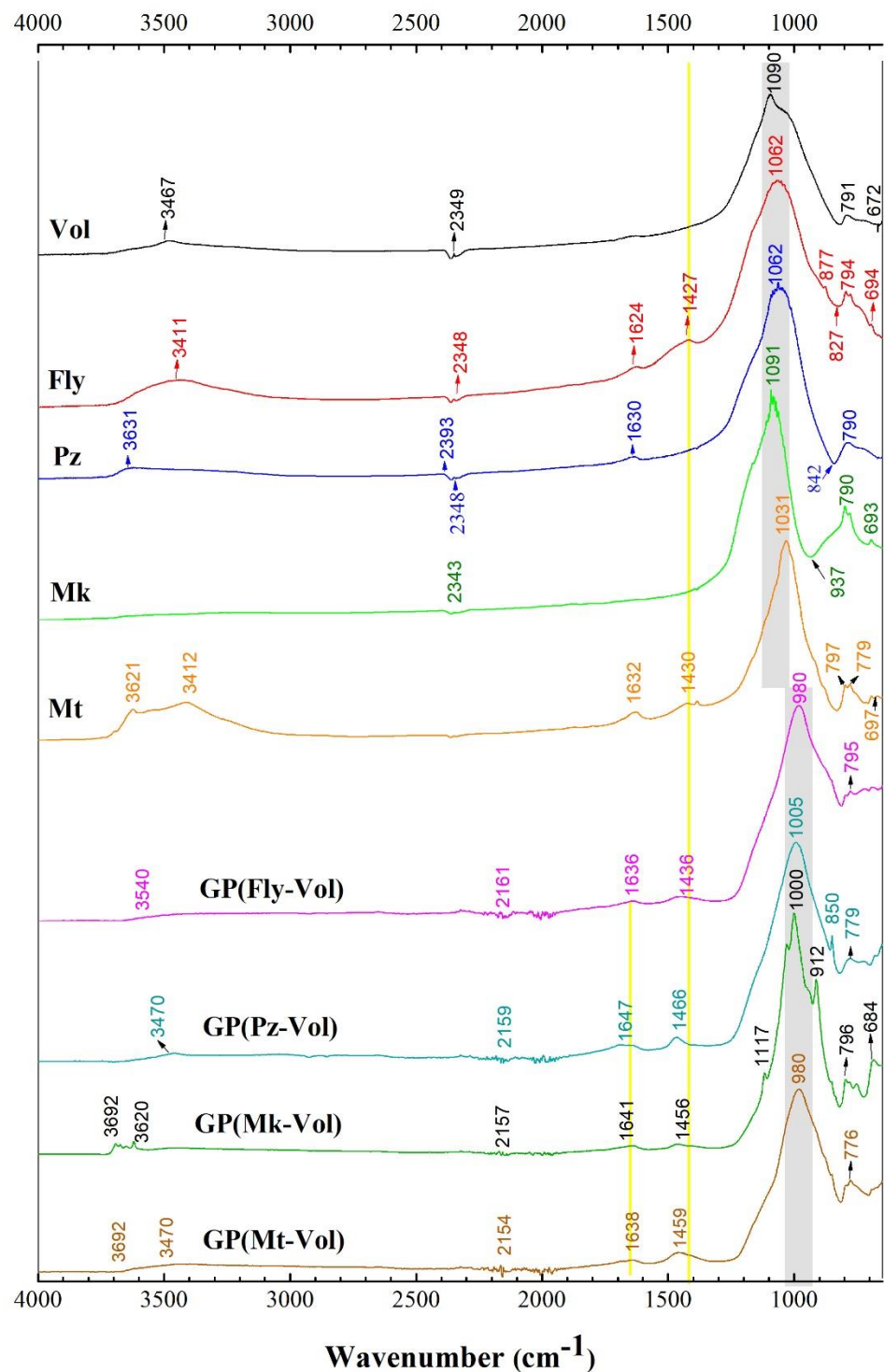
Figure 3. FTIR spectra of geopolymers based on volcanic ash and all raw materials (Fly, Pz, Mk, and Mt).

Moreover, the spectra show bands related to the vibration of carbonate ions (CO_3^{2-}) with a wave number of 1426 cm^{-1}, making its presence more noticeable in Fly and Mt samples, which could be attributed to the reaction of NaOH with CO_2 from the air [28]. It is clearly seen that, after the geopolymerization, the intensity of those bands decreases, and they shift to slightly higher wavenumbers. The weak absorption band at 797 cm^{-1} is related to the vibration of the symmetric stretching of the Si-O-Si bonds [37,38]. The broadbands located from 3400–3600 cm^{-1} are related to the stretching of -OH, while bands located in 1634–1664 cm^{-1} are related to the bending of the H-O-H groups. These bands

could represent the absorption of water trapped in the samples or water placed on the surface of the geopolymers [37,38].

3.3. Compression Strength

The results of the compression strength of geopolymers based on different combinations of raw materials (Fly-Vol, Pz-Vol, Mk-Vol, Mt-Vol) are shown in Figure 4. According to Figure 4 and the intensity of the diffuse halo peak in the XRD patterns (Figure 2), the mechanical strength of the geopolymer GP(Pz-Vol) is the highest, followed by GP(Mk-Vol), GP(Fly-Vol), and GP(Mt-Vol), because the high degree of amorphous phases existent in the prime materials improved the compression strength of geopolymers in comparison to those without the presence of a diffuse halo [2,39]. Therefore, GP(Pz-Vol) geopolymer presents the highest compression strength value due to the degree of amorphous components and the high chemical reaction activity of Pz according to the XRD results (Figure 1B). These characteristics of Pz promote the dissolution of the aluminosilicate and accelerate the polycondensation in geopolymers [33,39]. Besides, according to Tchakoute Kouamo [2], the amorphous phase contained in the raw material influences the compressive strength results because amorphous phases dissolve more easily than crystalline phases during geopolymerization, since an important part of the reaction takes place at the liquid–particle interface; moreover, finer particles allow a higher surface area and a more reactive material.
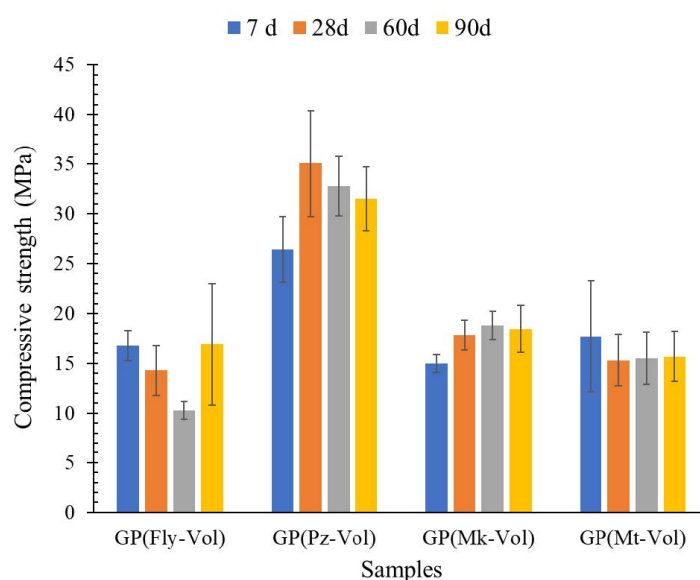

Figure 4. Compression strength of GP(Fly-Vol), GP(Pz-Vol), GP(Mk-Vol), and GP(Mt-Vol) geopolymers at 7, 28, 60, and 90 days of curing.

On the other hand, the compression strength of the GP(Pz-Vol) geopolymer after 7 days of curing is 26.4 MPa, then 35.1 MPa after 28 days of curing. This value obtained for the paste is even higher than the reported for Portland cement mortar (29.36 ± 2.57 MPa) [9], suggesting that a mortar made of GP(Pz-Vol) could even show better values. The compression strength after 60 days of curing is 32.8 MPa and finally 31.5 MPa after 90 days of curing. In addition, it was observed that the highest strength value was obtained at 28 days, then a slight decrease occurred indicating that the lack of sustainability of geopolymerization and solidification limits the growth of strength. This is probably because at longer times there is a greater loss of moisture and a small interaction of the remaining activating solution with the silicoaluminous components, which in turn could react with the carbon dioxide (CO_2) from the environment and lead to carbonation and generation of microcracks.

The strengths of the other pastes are lower, although the use of aggregates (mortar) could certainly increase them. The compressive strength of the geopolymer GP(Mk-Vol)

is 15 MPa after 7 days of curing, 17.8 MPa after 28 days, then it slightly increases to 18.8 after 60 days, and finally 18.4 MPa after 90 days. The raw material Mk has a particle size of 99.9991% under 38 μm, being the finest raw material employed in the production of geopolymers. This small particle size possibly affects the wettability that raw materials require, leading to an increase in the amount of activating solution in order to achieve a complete geopolymerization and, consequently, the found compressive strength is lower than expected. In addition, it is possible that the Mk forms interlocking pores (ion diffusion channels) in the geopolymer matrix. According to Kusbiantoro [40], the presence of pores in the initial stage of geopolymerization accelerates the efficiency in the transference of ions resulting in the improvement of the mechanical strength of geopolymers. As the reaction proceeds, free water in the capillary orifice evaporates to form air-filled holes. Additionally, while the geopolymer is destroyed by external stress, the holes transform themselves into a conduit for the propagation of microcracks, which reduces the mechanical strength of the geopolymers [37,40].

The GP(Mt-Vol) geopolymer has a compressive strength of 17.7 MPa after 7 days of curing, 15.3 MPa after 28 days, 15.5 MPa after 60 days, and 15.7 MPa after 90 days. Mt is the raw material with less amorphous components and bigger particle size. The XRD results indicate the partial solubility of the Mt and Vol components; however, the crystalline phases of the volcanic ash are still present in the GP(Mt-Vol) geopolymer diffractogram. These unreacted phases of Mt and Vol perform as microaggregates of the geopolymer, resulting in a compact and resistant structure [35]. The compressive strength of the GP(Fly-Vol) geopolymer is 16.8 MPa after 7 days of curing, 14.3 MPa after 28 days, 10.3 MPa after 60 days, and finally 16.9 MPa after 90 days. The fineness and water absorption of fly ash [40] reduce the water content in the geopolymer system. When the hydroxyl ion is quickly transferred into the fly ash particle, the dissolution of the aluminosilicates increases, as well as the gelation of the saturated aluminosilicate solution. However, the differences in the degree of solubility between fly ash and volcanic ash, as well as the variations in the wettability capacity of the activating solution, are due to the fineness of the fly ash, obtaining an unequal geopolymer gel production rate, and a decrease in the mechanical strength in geopolymers.

4. Conclusions

- It has been shown that it is possible to use mixtures of natural waste (volcanic ash), hazardous solid waste (fly ash and mining tailings), natural material (pozzolan), and metakaolin as raw materials for the production of geopolymers. According to XRD and FTIR analysis, the final products are identified as geopolymer compounds. Additionally, it has been seen that the combination of precursor materials has an influence on the geopolymerization, and the variation trend of the amorphous phase contained in the geopolymers was detected by qualitative XRD analysis.
- The FTIR analysis revealed that the main band located in the range of 1014–1042 cm^{-1} proves geopolymerization related to Si-O-Si (Al) bonds and the increase in the amount of SiO_2. The main band (related to N-A-S-H gel) shifts to a lower wavenumber. Additionally, it was observed that a change took place in the intensity and location in the range of 1417–1440 cm^{-1} of the groups related to the carbonate vibration which is probably detrimental to the mechanical properties that tend to cause cracks or micro-cracks on the geopolymer.
- The XRD analysis showed that the geopolymer composites have amorphous and semi-crystalline phases even in the raw materials that had crystalline phases. Among the four geopolymers, the GP(Pz-Vol) geopolymer had the highest amount of amorphous glassy phase, it has been seen that this promotes the development of the degree of geopolymerization and, therefore, the highest achieved mechanical strength. This is probably due to the unreacted phases that could act as microaggregates or fillers by reinforcing the geopolymer matrix, resulting in a compact and high-strength structure

- Additionally, a strong correlation was found between the strength values of the mortars and the SiO_2/Al_2O_3 ratios obtained from the precursor mixtures. Thus, the compressive strength of the GP(Pz-Vol) reached values of 35.1 MPa, with this mixture having a value of 7.09 SiO_2/Al_2O_3 ratio. This value obtained for GP(Pz-Vol) geopolymer is even higher than the reported for Portland cement mortar (29.36 $\pm$ 2.57 MPa), so this mortar could even show better values and applications.

Author Contributions: Conceptualization, R.C. and J.A.; methodology, J.A.; software, M.V.; validation, R.C., J.A. and M.V.; formal analysis, J.A.; investigation, R.C.; resources, Y.O.-V.; data curation, D.T.-Q.; writing—original draft preparation, F.V.; writing—review and editing, D.T.-Q.; visualization, J.T.-A.; supervision, F.V.; project administration, Y.O.-V.; funding acquisition, J.T.-A. All authors have read and agreed to the published version of the manuscript.

Conflicts of Interest: The authors declare no conflict of interest.

References

1. Davidovits, J. Geopolymers: Ceramic-like Inorganic Polymers. *J. Ceram. Sci. Technol.* **2017**, *8*, 335–350. [CrossRef]
2. Tchakoute Kouamo, H.; Elimbi, A.; Mbey, J.A.; Ngally Sabouang, C.J.; Njopwouo, D. The Effect of Adding Alumina-Oxide to Metakaolin and Volcanic Ash on Geopolymer Products: A Comparative Study. *Constr. Build. Mater.* **2012**, *35*, 960–969. [CrossRef]
3. Yunsheng, Z.; Wei, S.; Zongjin, L. Composition Design and Microstructural Characterization of Calcined Kaolin-Based Geopolymer Cement. *Appl. Clay Sci.* **2010**, *47*, 271–275. [CrossRef]
4. Rattanasak, U.; Chindaprasirt, P. Influence of NaOH Solution on the Synthesis of Fly Ash Geopolymer. *Miner. Eng.* **2009**, *22*, 1073–1078. [CrossRef]
5. Bondar, D.; Lynsdale, C.J.; Milestone, N.B.; Hassani, N.; Ramezanianpour, A.A. Effect of Adding Mineral Additives to Alkali-Activated Natural Pozzolan Paste. *Constr. Build. Mater.* **2011**, *25*, 2906–2910. [CrossRef]
6. Tekin, I. Properties of NaOH Activated Geopolymer with Marble, Travertine and Volcanic Tuff Wastes. *Constr. Build. Mater.* **2016**, *127*, 607–617. [CrossRef]
7. Churata, R.; Almirón, J.; Roudet, F.; Bautista, A.; Torres-Carrasco, M.; Tupayachy-Quispe, D. Influence of the Activating Solution on the Mechanical Properties of Compacted Volcanic Ash Based Geopolymers. *IOP Conf. Ser. Mater. Sci. Eng.* **2021**, *1150*, 012011. [CrossRef]
8. Tupayachy-Quispe, D.; Almirón, J.; Apaza, F.; Churata, R.; Paredes, E.; Torres-Carrasco, M.; Bautista, A. Peruvian Volcanic Ashes as New Alternative Material in Geopolymer Preparation: Influence of Dissolution Concentration and Wear Resistance. *Proc. LACCEI Int. Multi-Conf. Eng. Educ. Technol.* **2020**, 27–31. [CrossRef]
9. Calderón, N.; Vargas, M.; Almirón, J.; Bautista, A.; Velasco, F.; Tupayachy-Quispe, D. Influence of the Activating Solution and Aggregates in the Physical and Mechanical Properties of Volcanic Ash Based Geopolymer Mortars. *IOP Conf. Ser. Mater. Sci. Eng.* **2021**, *1054*, 012003. [CrossRef]
10. Ma, C.K.; Awang, A.Z.; Omar, W. Structural and Material Performance of Geopolymer Concrete: A Review. *Constr. Build. Mater.* **2018**, *186*, 90–102. [CrossRef]
11. Alnahhal, M.F.; Alengaram, U.J.; Jumaat, M.Z.; Abutaha, F.; Alqedra, M.A.; Nayaka, R.R. Assessment on Engineering Properties and CO2 Emissions of Recycled Aggregate Concrete Incorporating Waste Products as Supplements to Portland Cement. *J. Clean. Prod.* **2018**, *203*, 822–835. [CrossRef]
12. Amran, Y.H.M.; Alyousef, R.; Alabduljabbar, H.; El-Zeadani, M. Clean Production and Properties of Geopolymer Concrete; A Review. *J. Clean. Prod.* **2020**, *251*, 119679. [CrossRef]
13. Almutairi, A.L.; Tayeh, B.A.; Adesina, A.; Isleem, H.F.; Zeyad, A.M. Potential Applications of Geopolymer Concrete in Construction: A Review. *Case Stud. Constr. Mater.* **2021**, *15*, e00733. [CrossRef]
14. Song, D.; Huang, T.; Fang, Q.; Liu, A.; Gu, Y.F.; Liu, Y.Q.; Liu, L.F.; Zhang, S.W. Feasibility Exploration on the Geopolymerization Activation of Volcanic Tuff, Parametrical Optimization, and Reaction Mechanisms. *J. Mater. Res. Technol.* **2021**, *11*, 618–632. [CrossRef]
15. Roviello, G.; Ricciotti, L.; Tarallo, O.; Ferone, C.; Colangelo, F.; Roviello, V.; Cioffi, R. Innovative Fly Ash Geopolymer-Epoxy Composites: Preparation, Microstructure and Mechanical Properties. *Materials* **2016**, *9*, 461. [CrossRef] [PubMed]
16. Rakhimova, N.R.; Rakhimov, R.Z. Toward Clean Cement Technologies: A Review on Alkali-Activated Fly-Ash Cements Incorporated with Supplementary Materials. *J. Non-Cryst. Solids* **2019**, *509*, 31–41. [CrossRef]

17. Haddaji, Y.; Majdoubi, H.; Mansouri, S.; Tamraoui, Y.; el bouchti, M.; Manoun, B.; Oumam, M.; Hannache, H. Effect of Synthetic Fibers on the Properties of Geopolymers Based on Non-Heat Treated Phosphate Mine Tailing. *Mater. Chem. Phys.* **2021**, *260*, 124147. [CrossRef]

18. Awoyera, P.; Adesina, A. A Critical Review on Application of Alkali Activated Slag as a Sustainable Composite Binder. *Case Stud. Constr. Mater.* **2019**, *11*, e00268. [CrossRef]

19. Albidah, A.; Alghannam, M.; Abbas, H.; Almusallam, T.; Al-Salloum, Y. Characteristics of Metakaolin-Based Geopolymer Concrete for Different Mix Design Parameters. *J. Mater. Res. Technol.* **2021**, *10*, 84–98. [CrossRef]

20. Pradhan, P.; Panda, S.; Kumar Parhi, S.; Kumar Panigrahi, S. Factors Affecting Production and Properties of Self-Compacting Geopolymer Concrete—A Review. *Constr. Build. Mater.* **2022**, *344*, 128174. [CrossRef]

21. Atabey, İ.İ.; Karahan, O.; Bilim, C.; Atiş, C.D. The Influence of Activator Type and Quantity on the Transport Properties of Class F Fly Ash Geopolymer. *Constr. Build. Mater.* **2020**, *264*, 120268. [CrossRef]

22. Aygörmez, Y. Assessment of Performance of Metabentonite and Metazeolite-Based Geopolymers with Fly Ash Sand Replacement. *Constr. Build. Mater.* **2021**, *302*, 124423. [CrossRef]

23. Jamil, N.H.; al Bakri Abdullah, M.M.; Pa, F.C.; Mohamad, H.; Ibrahim, W.M.A.W.; Chaiprapa, J. Influences of SiO_2, Al_2O_3, CaO and MgO in Phase Transformation of Sintered Kaolin-Ground Granulated Blast Furnace Slag Geopolymer. *J. Mater. Res. Technol.* **2020**, *9*, 14922–14932. [CrossRef]

24. Zheng, L.; Wang, W.; Shi, Y. The Effects of Alkaline Dosage and Si/Al Ratio on the Immobilization of Heavy Metals in Municipal Solid Waste Incineration Fly Ash-Based Geopolymer. *Chemosphere* **2010**, *79*, 665–671. [CrossRef]

25. Hassan, A.; Arif, M.; Shariq, M. Use of Geopolymer Concrete for a Cleaner and Sustainable Environment – A Review of Mechanical Properties and Microstructure. *J. Clean. Prod.* **2019**, *223*, 704–728. [CrossRef]

26. Messina, F.; Ferone, C.; Colangelo, F.; Cioffi, R. Low Temperature Alkaline Activation of Weathered Fly Ash: Influence of Mineral Admixtures on Early Age Performance. *Constr. Build. Mater.* **2015**, *86*, 169–177. [CrossRef]

27. Çelikten, S.; Erdoğan, G. Effects of Perlite/Fly Ash Ratio and the Curing Conditions on the Mechanical and Microstructural Properties of Geopolymers Subjected to Elevated Temperatures. *Ceram. Int.* **2022**, *in press*. [CrossRef]

28. Amran, M.; Debbarma, S.; Ozbakkaloglu, T. Fly Ash-Based Eco-Friendly Geopolymer Concrete: A Critical Review of the Long-Term Durability Properties. *Constr. Build. Mater.* **2021**, *270*, 121857. [CrossRef]

29. Moussallam, Y.; Peters, N.; Masias, P.; Apaza, F.; Barnie, T.; Ian Schipper, C.; Curtis, A.; Tamburello, G.; Aiuppa, A.; Bani, P.; et al. Magmatic Gas Percolation through the Old Lava Dome of El Misti Volcano. *Bull. Volcanol.* **2017**, *79*, 1–11. [CrossRef]

30. Rivera, M.; Thouret, J.C.; Samaniego, P.; le Pennec, J.L. The 2006-2009 Activity of the Ubinas Volcano (Peru): Petrology of the 2006 Eruptive Products and Insights into Genesis of Andesite Magmas, Magma Recharge and Plumbing System. *J. Volcanol. Geotherm. Res.* **2014**, *270*, 122–141. [CrossRef]

31. Rivera, M.; Thouret, J.C.; Mariño, J.; Berolatti, R.; Fuentes, J. Characteristics and Management of the 2006-2008 Volcanic Crisis at the Ubinas Volcano (Peru). *J. Volcanol. Geotherm. Res.* **2010**, *198*, 19–34. [CrossRef]

32. Yadav, A.L.; Sairam, V.; Srinivasan, K.; Muruganandam, L. Synthesis and Characterization of Geopolymer from Metakaolin and Sugarcane Bagasse Ash. *Constr. Build. Mater.* **2020**, *258*, 119231. [CrossRef]

33. Liu, X.; Jiang, J.; Zhang, H.; Li, M.; Wu, Y.; Guo, L.; Wang, W.; Duan, P.; Zhang, W.; Zhang, Z. Thermal Stability and Microstructure of Metakaolin-Based Geopolymer Blended with Rice Husk Ash. *Appl. Clay Sci.* **2020**, *196*, 105769. [CrossRef]

34. Zain, M.F.M.; Islam, M.N.; Mahmud, F.; Jamil, M. Production of Rice Husk Ash for Use in Concrete as a Supplementary Cementitious Material. *Constr. Build. Mater.* **2011**, *25*, 798–805. [CrossRef]

35. Sontia Metekong, J.V.; Kaze, C.R.; Deutou, J.G.; Venyite, P.; Nana, A.; Kamseu, E.; Melo, U.C.; Tatietse, T.T. Evaluation of Performances of Volcanic-Ash-Laterite Based Blended Geopolymer Concretes: Mechanical Properties and Durability. *J. Build. Eng.* **2021**, *34*, 101935. [CrossRef]

36. Ahmari, S.; Zhang, L. Utilization of Cement Kiln Dust (CKD) to Enhance Mine Tailings-Based Geopolymer Bricks. *Constr. Build. Mater.* **2013**, *40*, 1002–1011. [CrossRef]

37. Yaseri, S.; Masoomi Verki, V.; Mahdikhani, M. Utilization of High Volume Cement Kiln Dust and Rice Husk Ash in the Production of Sustainable Geopolymer. *J. Clean. Prod.* **2019**, *230*, 592–602. [CrossRef]

38. Sore, S.O.; Messan, A.; Prud'homme, E.; Escadeillas, G.; Tsobnang, F. Synthesis and Characterization of Geopolymer Binders Based on Local Materials from Burkina Faso – Metakaolin and Rice Husk Ash. *Constr. Build. Mater.* **2016**, *124*, 301–311. [CrossRef]

39. Liang, G.; Zhu, H.; Zhang, Z.; Wu, Q. Effect of Rice Husk Ash Addition on the Compressive Strength and Thermal Stability of Metakaolin Based Geopolymer. *Constr. Build. Mater.* **2019**, *222*, 872–881. [CrossRef]

40. Kusbiantoro, A.; Nuruddin, M.F.; Shafiq, N.; Qazi, S.A. The Effect of Microwave Incinerated Rice Husk Ash on the Compressive and Bond Strength of Fly Ash Based Geopolymer Concrete. *Constr. Build. Mater.* **2012**, *36*, 695–703. [CrossRef]